

Phases of QCD at High Baryon Density

Thomas Schäfer^{1,2} and Edward Shuryak¹

¹ Department of Physics and Astronomy, State University of New York, Stony Brook, NY 11794-3800

² Riken-BNL Research Center, Brookhaven National Laboratory, Upton, NY 11973

Abstract. We review recent work on the phase structure of QCD at very high baryon density. We introduce the phenomenon of color superconductivity and discuss how the quark masses and chemical potentials determine the structure of the superfluid quark phase. We comment on the possibility of kaon condensation at very high baryon density and study the competition between superfluid, density wave, and chiral crystal phases at intermediate density.

1 Color Superconductivity

In the interior of compact stars matter is compressed to densities several times larger than the density of ordinary matter. Unlike the situation in relativistic heavy ion collisions, these conditions are maintained for essentially infinite periods of time. Also, compared to QCD scales, matter inside a compact star is quite cold. At low density quarks are confined, chiral symmetry is broken, and baryonic matter is described in terms of neutrons and protons as well as their excitations. At very large density, on the other hand, we expect that baryonic matter is described more effectively in terms of quarks rather than hadrons. As we shall see, these quarks can form new condensates and the phase structure of dense quark matter is quite rich.

At very high density the natural degrees of freedom are quark excitations and holes in the vicinity of the Fermi surface. Since the Fermi momentum is large, asymptotic freedom implies that the interaction between quasi-particles is weak. In QCD, because of the presence of unscreened long range gauge forces, this is not quite true. Nevertheless, we believe that this fact does not essentially modify the argument. We know from the theory of superconductivity the Fermi surface is unstable in the presence of even an arbitrarily weak attractive interaction. At very large density, the attraction is provided by one-gluon exchange between quarks in a color anti-symmetric $\bar{3}$ state. High density quark matter is therefore expected to be a color superconductor [1,2,3,4].

Color superconductivity is described by a pair condensate of the form

$$\phi = \langle \psi^T C \Gamma_D \lambda_C \tau_F \psi \rangle. \quad (1)$$

Here, C is the charge conjugation matrix, and $\Gamma_D, \lambda_C, \tau_F$ are Dirac, color, and flavor matrices. Except in the case of only two colors, the order parameter cannot be a color singlet. Color superconductivity is therefore characterized by the

breakdown of color gauge invariance. As usual, this statement has to be interpreted with care because local gauge invariance cannot really be broken. Nevertheless, we can study gauge invariant consequences of a quark pair condensate, in particular the formation of a gap in the excitation spectrum.

In addition to that, color superconductivity can lead to the breakdown of global symmetries. We shall see that in some cases there is a gauge invariant order parameter for the $U(1)$ of baryon number. This corresponds to true superfluidity and the appearance of a massless phonon. We shall also find that for $N_f > 2$ color superconductivity leads to chiral symmetry breaking and that quark matter may support a kaon condensate. Finally, as we move to stronger coupling we find that other forms of order can compete with color superconductivity and that quark matter may exist in the form of chiral density waves or chiral crystals.

2 Phase Structure in Weak Coupling

2.1 QCD with two flavors

In this section we shall discuss how to use weak coupling methods in order to explore the phases of dense quark matter. We begin with what is usually considered to be the simplest case, quark matter with two degenerate flavors, up and down. Renormalization group arguments suggest [5,6,7], and explicit calculations show [8,9], that whenever possible quark pairs condense in an s -wave. This means that the spin wave function of the pair is anti-symmetric. Since the color wave function is also anti-symmetric, the Pauli principle requires the flavor wave function to be anti-symmetric, too. This essentially determines the structure of the order parameter [10,11]

$$\phi^a = \langle \epsilon^{abc} \psi^b C \gamma_5 \tau_2 \psi^c \rangle. \quad (2)$$

This order parameter breaks the color $SU(3) \rightarrow SU(2)$ and leads to a gap for up and down quarks with two out of the three colors. Chiral and isospin symmetry remain unbroken.

We can calculate the magnitude of the gap and the condensation energy using weak coupling methods. In weak coupling the gap is determined by ladder diagrams with the one gluon exchange interaction. These diagrams can be summed using the gap equation [12,13,14,15,16]

$$\Delta(p_0) = \frac{g^2}{12\pi^2} \int dq_0 \int d\cos\theta \left(\frac{\frac{3}{2} - \frac{1}{2} \cos\theta}{1 - \cos\theta + G/(2\mu^2)} + \frac{\frac{1}{2} + \frac{1}{2} \cos\theta}{1 - \cos\theta + F/(2\mu^2)} \right) \frac{\Delta(q_0)}{\sqrt{q_0^2 + \Delta(q_0)^2}}. \quad (3)$$

Here, $\Delta(p_0)$ is the frequency dependent gap, g is the QCD coupling constant and G and F are the self energies of magnetic and electric gluons. This gap equation is very similar to the BCS gap equations that describe nuclear superfluids. The main difference is that because the gluon is massless, the gap equation contains

a collinear divergence for $\cos\theta \rightarrow 1$. In a dense medium the collinear divergence is regularized by the gluon self energy. For $\mathbf{q} \rightarrow 0$ and to leading order in perturbation theory we have

$$F = 2m^2, \quad G = \frac{\pi}{2} m^2 \frac{q_0}{|\mathbf{q}|}, \quad (4)$$

with $m^2 = N_f g^2 \mu^2 / (4\pi^2)$. In the electric part, $m_D^2 = 2m^2$ is the familiar Debye screening mass. In the magnetic part, there is no screening of static modes, but non-static modes are dynamically screened due to Landau damping.

We can now perform the angular integral and find

$$\Delta(p_0) = \frac{g^2}{18\pi^2} \int dq_0 \log\left(\frac{b\mu}{|p_0 - q_0|}\right) \frac{\Delta(q_0)}{\sqrt{q_0^2 + \Delta(q_0)^2}}, \quad (5)$$

with $b = 256\pi^4 (2/N_f)^{5/2} g^{-5}$. This result shows why it was important to keep the frequency dependence of the gap. Because the collinear divergence is regulated by dynamic screening, the gap equation depends on p_0 even if the frequency is small. We can also see that the gap scales as $\exp(-c/g)$. The collinear divergence leads to a gap equation with a double-log behavior. Qualitatively

$$1 \sim \frac{g^2}{18\pi^2} \left[\log\left(\frac{\mu}{\Delta}\right) \right]^2, \quad (6)$$

from which we conclude that $\Delta \sim \exp(-c/g)$. The approximation (6) is not sufficiently accurate to determine the correct value of the constant c . A more detailed analysis shows that the gap on the Fermi surface is given by

$$\Delta_0 \simeq 512\pi^4 (2/N_f)^{5/2} \mu g^{-5} \exp\left(-\frac{3\pi^2}{\sqrt{2}g}\right). \quad (7)$$

We should emphasize that, strictly speaking, this result contains only an estimate of the pre-exponent. It was recently argued that wave function renormalization and quasi-particle damping give $O(1)$ contributions to the pre-exponent which substantially reduce the gap [16].

For chemical potentials $\mu < 1$ GeV, the coupling constant is not small and the applicability of perturbation theory is in doubt. If we ignore this problem and extrapolate the perturbative calculation to densities $\rho \simeq 5\rho_0$ we find gaps $\Delta \simeq 100$ MeV. This result may indeed be more reliable than the calculation on which it is based. In particular, we note that similar results have been obtained using realistic interactions which reproduce the chiral condensate at zero baryon density [10,11].

We can also determine the condensation energy. In weak coupling the grand potential can be calculated from [4]

$$\Omega = \frac{1}{2} \int \frac{d^4q}{(2\pi)^4} \left\{ -\text{tr} [S(q)\Sigma(q)] + \text{tr} [S_0^{-1}(q)S(q)] \right\}, \quad (8)$$

where $S(q)$ and $\Sigma(q)$ are the Nambu-Gorkov propagator and proper self energy. Using the propagator in the superconducting phase we find

$$\epsilon = 4 \frac{\mu^2}{4\pi^2} \Delta_0^2 \log \left(\frac{\Delta_0}{\mu} \right), \quad (9)$$

where the factor $4 = 2N_f$ comes from the number of condensed species. Using $\Delta_0 \simeq 100$ MeV and $\mu \simeq 500$ MeV we find $\epsilon \simeq -50$ MeV/fm³. This shows that the condensation energy is only a small $O(\Delta^2/\mu^2)$ correction to the total energy density of the quark phase. We note that the result for the condensation energy agrees with BCS theory. The same is true for the critical temperature which is given by $T_c = 0.56\Delta_0$.

2.2 QCD with three flavors: Color-Flavor-Locking

If quark matter is formed at densities several times nuclear matter density we expect the quark chemical potential to be larger than the strange quark mass. We therefore have to determine the structure of the superfluid order parameter for three quark flavors. We begin with the idealized situation of three degenerate flavors. From the arguments given in the last section we expect the order parameter to be color and flavor anti-symmetric matrix of the form

$$\phi_{ij}^{ab} = \langle \psi_i^a C \gamma_5 \psi_j^b \rangle. \quad (10)$$

In order to determine the precise structure of this matrix we have to extremize grand canonical potential. We find [17,18]

$$\Delta_{ij}^{ab} = \Delta(\delta_i^a \delta_j^b - \delta_i^b \delta_j^a), \quad (11)$$

which describes the color-flavor locked phase proposed in [19]. Both color and flavor symmetry are completely broken. There are eight combinations of color and flavor symmetries that generate unbroken global symmetries. The symmetry breaking pattern is

$$SU(3)_L \times SU(3)_R \times U(1)_V \rightarrow SU(3)_V. \quad (12)$$

This is exactly the same symmetry breaking that QCD exhibits at low density. The spectrum of excitations in the color-flavor-locked (CFL) phase also looks remarkably like the spectrum of QCD at low density [20]. The excitations can be classified according to their quantum numbers under the unbroken $SU(3)$, and by their electric charge. The modified charge operator that generates a true symmetry of the CFL phase is given by a linear combination of the original charge operator Q_{em} and the color hypercharge operator $Q = \text{diag}(-2/3, -2/3, 1/3)$. Also, baryon number is only broken modulo $2/3$, which means that one can still distinguish baryons from mesons. We find that the CFL phase contains an octet of Goldstone bosons associated with chiral symmetry breaking, an octet of vector mesons, an octet and a singlet of baryons, and a singlet Goldstone boson related to superfluidity. All of these states have integer charges.

With the exception of the $U(1)$ Goldstone boson, these states exactly match the quantum numbers of the lowest lying multiplets in QCD at low density. In addition to that, the presence of the $U(1)$ Goldstone boson can also be understood. The $U(1)$ order parameter is $\langle(uds)(uds)\rangle$. This order parameter has the quantum numbers of a 0^+ $\Lambda\Lambda$ pair condensate. In $N_f = 3$ QCD, this is the most symmetric two nucleon channel, and a very likely candidate for superfluidity in nuclear matter at low to moderate density. We conclude that in QCD with three degenerate light flavors, there is no fundamental difference between the high and low density phases. This implies that a low density hyper-nuclear phase and the high density quark phase might be continuously connected, without an intervening phase transition.

2.3 QCD with one flavor: Color-Spin-Locking

In this section we shall study superfluid quark matter with only one quark flavor. As we will discuss in more detail in the next section, our results are relevant to quark matter with two or three flavors. This is the case when the Fermi surfaces of the individual flavors are too far apart in order to allow for pairing between different species.

If two quarks with the same flavor are in a color anti-symmetric wave function then their combined spin and spatial wave function cannot be antisymmetric. This means that pairing between identical flavors has to involve total angular momentum one or greater. The simplest order parameters are of the form

$$\Phi_1 = \langle \epsilon^{3ab} \psi^a C \gamma \psi^b \rangle, \quad \Phi_2 = \langle \epsilon^{3ab} \psi^a C \hat{q} \psi^b \rangle. \quad (13)$$

The corresponding gaps can be determined using the methods introduced in section 2.1. We find $\Delta(\Phi_{1,2}) = \exp(-3c_{1,2})\Delta_0$ with $c_1 = -1.5$ and $c_2 = -2$ [8,9]. While the natural scale of the s-wave gap is $\Delta = 100$ MeV, the p-wave gap is expected to be less than 1 MeV.

The spin one order parameter (13) is a color-spin matrix. This opens the possibility that color and spin degrees become entangled, similar to the color-flavor locked phase (11) or the B-phase of liquid ${}^3\text{He}$. The corresponding order parameter is

$$\Phi_{CSL} = \delta_i^a \langle \epsilon^{abc} \psi^b C (\cos(\beta)\hat{q}_i + \sin(\beta)\gamma_i) \psi^c \rangle, \quad (14)$$

where the angle β determines the mixing between the two types of condensates shown in (13). In reference [9] we showed that the color-spin locked phase (14) is favored over the ‘‘polar’’ phase (13).

In the color-spin locked phase color and rotational invariance are broken, but a diagonal $SO(3)$ survives. As a consequence, the gap is isotropic. There are no gapless modes except if β takes on special values. The parameter β is sensitive to the quark mass and to higher order corrections. In the non-relativistic limit we find $\beta = \pi/4$ whereas in the ultra-relativistic limit $\beta = \pi/2$.

3 The Role of the Strange Quark Mass and the Electron Chemical Potential

So far, we have only considered the case of two or three degenerate quark flavors. In the real world, the strange quark is significantly heavier than the up and down quarks. Also, in the interior of a neutron star, electrons are present and the chemical potentials for up and down quarks are not equal.

The role of the strange quark mass in the high density phase was studied in [21,22]. The main effect is a purely kinematic phenomenon that is easily explained. The Fermi surface for the strange quarks is shifted by $\delta p_F = \mu - (\mu^2 - m_s^2)^{1/2} \simeq m_s^2/(2\mu)$ with respect to the Fermi surface of the light quarks. The condensate involves pairing between quarks of different flavors at opposite points on the Fermi surface. But if the Fermi surfaces are shifted, then the pairs do not have total momentum zero, and they cannot mix with pairs at others points on the Fermi surface. If the system is superfluid then the Fermi surface is smeared out over a range Δ . This means that pairing between strange and light quarks can take place as long as the mismatch between the Fermi momenta is smaller than the gap,

$$\Delta > \frac{m_s^2}{2\mu}. \quad (15)$$

This conclusion is supported by a more detailed analysis [21,22]. Since flavor symmetry is broken, we allow the $\langle ud \rangle$ and $\langle us \rangle = \langle ds \rangle$ components of the CFL condensate to be different. The $N_f = 2$ phase corresponds to $\langle us \rangle = \langle ds \rangle = 0$. We find that there is a first order phase transition from the CFL to the $N_f = 2$ phase, and that the critical strange quark mass is in rough agreement with the estimate (15).

For densities $\rho \simeq (5-10)\rho_0$ the critical strange quark mass is close to physical mass of the strange quark. It is therefore hard to predict with certainty whether superconducting strange quark matter in the interior of a neutron star is in the color-flavor locked phase. Neutron star observations may help to answer the question. In the CFL phase all quarks have large gaps, whereas in the unlocked phase up and down quarks of the first two colors have large gaps, strange quarks have a small gap, and the up and down quarks of the remaining color have tiny gaps, or may not be gapped at all.

The effects of a non-zero electron chemical potential was studied in [23]. If the electron chemical potential exceeds the gap in the up-down sector then up and down quarks cannot pair. In this case, the up and down quarks pair separately, and with much smaller gaps, in the one flavor phase discussed in section 14. Between the phases with $\langle ud \rangle$ and $\langle uu \rangle, \langle dd \rangle$ pairing there is a small window of electron chemical potentials where inhomogeneous superconductivity takes place [24].

4 Kaon Condensation

The low energy properties of dense quark matter are determined by collective modes. In the color-flavor locked phase these modes are the phonon and the pseudoscalar Goldstone bosons, the pions, kaons and etas. Some time ago, it was suggested that pions [25,26,27] or kaons [28,29] might form Bose condensates in dense baryonic matter. The proposed critical densities were close to nuclear matter density in the case of pion condensation, and several times nuclear matter density in the case of kaon condensation. Since mesonic modes persist in the color-flavor-locked phase of quark matter, we can now revisit the issue of Goldstone boson condensation [30]. In particular, we shall be able to use rigorous weak coupling methods in order to address the possibility of Bose condensation in dense matter.

Our starting point is the effective lagrangian for the pseudoscalar Goldstone in dense matter [31,32]

$$\mathcal{L}_{eff} = \frac{f_\pi^2}{4} \text{Tr} [\partial_0 \Sigma \partial_0 \Sigma^\dagger + v_\pi^2 \partial_i \Sigma \partial_i \Sigma^\dagger] - c [\det(M) \text{Tr}(M^{-1} \Sigma) + h.c.]. \quad (16)$$

Here, $\Sigma \in SU(3)$ is the Goldstone boson field, v_π is the velocity of the Goldstone modes and $M = \text{diag}(m_u, m_d, m_s)$ is the quark mass matrix. The effective description is valid for energies and momenta below the scale set by the gap, $\omega, q \ll \Delta$. The low energy constants can be determined in weak coupling perturbation theory. The result is $v_\pi^2 = 1/3$ and [32,33,34,35,36]

$$f_\pi^2 = \frac{21 - 8 \log(2)}{18} \frac{\mu^2}{2\pi^2}, \quad (17)$$

$$c = \frac{3\Delta^2}{2\pi^2} \cdot \frac{2}{f_\pi^2}. \quad (18)$$

We can now determine the masses of the Goldstone bosons

$$m_{\pi^\pm} = c(m_u + m_d)m_s, \quad m_{K^\pm} = cm_d(m_u + m_s). \quad (19)$$

This result shows that the kaon is *lighter* than the pion. This can be understood from the fact that, at high density, it is more appropriate to think of the interpolating field Σ as

$$\Sigma_{ij} \sim \epsilon_{ikl} \epsilon_{jmn} \bar{\psi}_{L,k} \bar{\psi}_{L,l} \psi_{R,m} \psi_{R,n} \quad (20)$$

rather than the more familiar $\Sigma_{ij} \sim \bar{\psi}_{L,i} \psi_{R,j}$ [31]. Using (20) we observe that the negative pion field has the flavor structure $\bar{d}\bar{s}us$ and therefore has mass proportional to $(m_u + m_d)m_s$ [32]. Putting in numerical values we find that the kaon mass is very small, $m_{K^-} \simeq 5$ MeV at $\mu = 500$ MeV and $m_{K^-} \simeq 1$ MeV at $\mu = 1000$ MeV.

There are two reasons why the pseudoscalar Goldstone bosons are anomalously light. First of all, the Goldstone boson masses in the color-flavor-locked

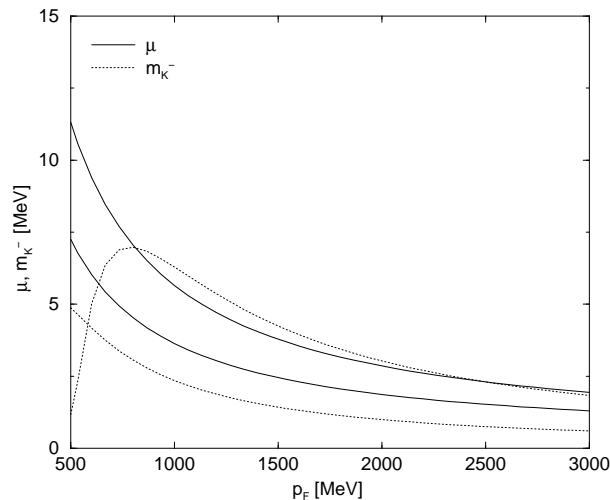


Fig. 1. Electron chemical potential (solid lines) and kaon mass (dashed lines) in the color-flavor-locked quark phase. The two curves for both quantities represent a simple estimate of the uncertainties due to the value of the strange quark mass and the scale setting procedure.

phase are proportional to the quark masses squared rather than linear in the quark mass, as they are at zero density. This is due to an approximate Z_2 chiral symmetry in the color-flavor-locked phase [19]. In addition to that, the Goldstone boson masses are suppressed by a factor Δ/μ . This is a consequence of the fact that the Goldstone modes are collective excitations of particles and holes near the Fermi surface, whereas the quark mass term connects particles and anti-particles, far away from the Fermi surface.

The fact that the meson spectrum is inverted, and that the kaon mass is exceptionally small opens the possibility that in dense quark matter electrons decay into kaons, and a kaon condensate is formed. Consider a kaon condensate $\langle K^- \rangle = v_K e^{-i\mu t}$ where μ is the chemical potential for negative charge. The thermodynamic potential $\mathcal{H} - \mu Q$ for this state is given by

$$\begin{aligned} \epsilon(\rho_q, x, y, \mu) = & \frac{3}{4\pi^2} \pi^{8/3} \rho_q^{4/3} \left\{ x^{4/3} + y^{4/3} + (1-x-y)^{4/3} \right. \\ & \left. + \pi^{-4/3} \rho_q^{-2/3} m_s^2 (1-x-y)^{2/3} \right\} \\ & - (\mu^2 - m_K^2) v_K^2 + O(v_K^3) + \mu \rho_q x - \frac{1}{12\pi^2} \mu^4 \end{aligned} \quad (21)$$

Here, $\rho_q = 3\rho_B$ is the quark density, and $x = \rho_u/\rho_q$ and $y = \rho_d/\rho_q$ are the up and down quark fractions. For simplicity, we have dropped higher order terms in

the strange quark mass and neglected the electron mass. In order to determine the ground state we have to make (21) stationary with respect to x, y, μ and v_K . Minimization with respect to x and y enforces β equilibrium, while minimization with respect to μ ensures charge neutrality. Below the onset for kaon condensation we have $v_K = 0$ and there is no kaon contribution to the charge density. Neglecting m_e and higher order corrections in m_s we find

$$\mu \simeq \frac{m_s^2}{4p_F} = \frac{\pi^{2/3} m_s^2}{4\rho_B^{1/3}}. \quad (22)$$

In the absence of kaon condensation, the electron chemical potential will level off at the value of the electron mass for very high baryon density. The onset of kaon condensation is determined by the condition $\mu = m_K$. At this point it becomes favorable to convert electrons into negatively charged kaons.

Results for the electron chemical potential and the kaon mass as a function of the light quark Fermi momentum are shown in Fig. 1. In order to assess some of the uncertainties we have varied the quark masses in the range $m_u = (3-5)$ MeV, $m_d = (6-8)$ MeV, and $m_s = (120-150)$ MeV. We have used the one loop result for the running coupling constant at two different scales $q = \mu$ and $q = \mu/2$. The scale parameter was set to $\Lambda_{QCD} = 238$ MeV, corresponding to $\alpha_s(m_\tau) = 0.35$. An important constraint is provided by the condition $m_s < \sqrt{2p_F\Delta}$ discussed in the previous section. We have checked that this condition is always satisfied for $p_F > 500$ MeV. Figure 1 shows that there is significant uncertainty in the relative magnitude of the chemical potential and the kaon mass. Nevertheless, the band of kaon mass predictions lies systematically below the predicted chemical potentials. We therefore conclude that kaon condensation appears likely even for moderate Fermi momenta $p_F \simeq 500$ MeV. For very large baryon density $\mu \rightarrow m_e$ while $m_K \rightarrow 0$ and kaon condensation seems inevitable.

5 Chiral Waves and Chiral Crystals

It is very important for the structure of compact stars to determine whether the quark matter core is in liquid or solid form. In the previous sections we discussed the case of weak coupling. In this case, particle-particle pairing is the only instability that needs to be considered. Nevertheless, in strong coupling, or if superconductivity is suppressed, other forms of pairing may take place. Obvious candidates are the formation of larger clusters or particle-hole pairing.

Particle-hole pairing is characterized by an order parameter of the form

$$\langle \bar{\psi}(x)\psi(y) \rangle = \exp(i\mathbf{Q} \cdot (\mathbf{x} + \mathbf{y}))\Sigma(x - y), \quad (23)$$

where \mathbf{Q} is an arbitrary vector. This state describes a chiral density wave. It was first suggested in [37] as the ground state of QCD at large chemical potential and large N_c . This suggestion was based on the fact that particle-particle pairing, and superconductivity, is suppressed for large N_c whereas particle-hole pairing is not. Particle-hole pairing, on the other hand, uses only a small part of the Fermi

surface and does not take place in weak coupling. In the case of the one-gluon exchange interaction these issues were studied in [38]. The main conclusion is that, in weak coupling, the chiral density wave instability requires very large $N_c \gg 3$.

At moderate densities, and using realistic interactions, this is not necessarily the case. In particular, we know that at zero density the particle-anti-particle interaction is stronger, by a factor $N_c - 2$, than the particle-particle interaction. In a Nambu-Jona-Lasinio type description this interaction exceeds the critical value required for chiral symmetry breaking to take place. For this reason we have recently studied the competition between the particle-particle and particle-hole instabilities using non-perturbative, instanton generated, forces [39]. Our results are not only relevant to flavor symmetric quark matter at moderate densities, but also for the important case when there is a substantial difference between the chemical potentials for up and down quarks. As discussed in section 3 this disfavors ud -pairing, but it does not inhibit uu^{-1} and dd^{-1} particle-hole pairing.

Our results show that at low density the chiral density wave state is practically degenerate with the BCS solution. Given the uncertainties that affect the calculation this implies that both states have to be considered as realistic possibilities for the behavior of quark matter near the phase transition.

5.1 BCS Pairing

In order to study competing instabilities we use the standard Nambu-Gorkov formalism, in which the propagator is written as a matrix in the space of all possible pair condensates. The BCS channel is described by the 2×2 matrix

$$\hat{G}_{BCS} = \begin{pmatrix} \langle c_{k\uparrow} c_{k\uparrow}^\dagger \rangle & \langle c_{k\uparrow} c_{-k\downarrow} \rangle \\ \langle c_{-k\downarrow}^\dagger c_{k\uparrow}^\dagger \rangle & \langle c_{-k\downarrow}^\dagger c_{-k\downarrow} \rangle \end{pmatrix} \equiv \begin{pmatrix} G(k_0, \mathbf{k}, \Delta) & \bar{F}(k_0, \mathbf{k}, \Delta) \\ F(k_0, \mathbf{k}, \Delta) & \bar{G}(k_0, -\mathbf{k}, \Delta) \end{pmatrix}. \quad (24)$$

The propagator has the form

$$\hat{G}_{BCS} = \frac{1}{G_0^{-1} \bar{G}_0^{-1} - \Delta \bar{\Delta}} \begin{pmatrix} \bar{G}_0^{-1} & -\Delta \\ -\Delta & G_0^{-1} \end{pmatrix}, \quad (25)$$

where

$$G_0 = \frac{1}{k_0 - \epsilon_k + i\delta_{\epsilon_k}}, \quad \bar{G}_0 = \frac{1}{k_0 + \epsilon_k + i\delta_{\epsilon_k}} \quad (26)$$

are the free particle propagator and its conjugate at finite chemical potential. Here, $\epsilon_k = \omega_k - \mu_q$ and $\delta_{\epsilon_k} = \text{sgn}(\epsilon_k)\delta$ determines the pole position. From this equation we can read off the diagonal and off-diagonal components of the Gorkov propagator. The off-diagonal, anomalous, propagator is

$$F(k_0, \mathbf{k}, \Delta) = \frac{-\Delta}{(k_0 - \epsilon_k + i\delta_{\epsilon_k})(k_0 + \epsilon_k + i\delta_{\epsilon_k}) - \Delta^2}. \quad (27)$$

The anomalous self energy Δ is determined by the gap equation

$$\Delta = (-i) \alpha_{pp} \int \frac{d^4 p}{(2\pi)^4} F(p_0, \mathbf{p}, \Delta). \quad (28)$$

Here α_{pp} is the effective coupling in the particle-particle channel.

5.2 Chiral Density Wave

Using the same formalism we can also address pairing in the particle-hole channel at finite total pair momentum Q . In the mean-field approximation, the full Greens function in the presence of a single density wave takes the form

$$\begin{aligned} \hat{G}_{Ovh} &= \begin{pmatrix} \langle c_{k\uparrow} c_{k\uparrow}^\dagger \rangle & \langle c_{k\uparrow} c_{k+Q\downarrow}^\dagger \rangle \\ \langle c_{k+Q\downarrow} c_{k\uparrow}^\dagger \rangle & \langle c_{k+Q\downarrow} c_{k+Q\downarrow}^\dagger \rangle \end{pmatrix} \equiv \begin{pmatrix} G(k_0, \mathbf{k}, \mathbf{Q}, \sigma) & \bar{S}(k_0, \mathbf{k}, \mathbf{Q}, \sigma) \\ S(k_0, \mathbf{k}, \mathbf{Q}, \sigma) & G(k_0, \mathbf{k} + \mathbf{Q}, \mathbf{Q}, \sigma) \end{pmatrix} \\ &= [\hat{G}_0^{-1} - \hat{\sigma}]^{-1} \end{aligned} \quad (29)$$

Again, we can read off the anomalous part of the Greens function

$$S(k_0, \mathbf{k}, \mathbf{Q}, \sigma) = \frac{-\sigma}{(k_0 - \epsilon_k + i\delta_{\epsilon_k})(k_0 - \epsilon_{k+Q} + i\delta_{\epsilon_{k+Q}}) - \sigma^2}, \quad (30)$$

and the anomalous self energy σ is determined by a self-consistency, or gap, equation

$$\sigma = (-i)\alpha_{ph} \int \frac{d^4 p}{(2\pi)^4} S(p_0, \mathbf{p}, \mathbf{Q}, \sigma; \mu_q). \quad (31)$$

Notice that the energy contour integration receives non-vanishing contributions only if

$$\epsilon_p \epsilon_{p+Q} - \sigma^2 < 0, \quad (32)$$

which ensures that the two poles in p_0 are in different (upper/lower) half-planes. This means that one particle (above the Fermi surface) and one hole (below the Fermi surface) participate in the interaction.

The formation of a condensate carrying nonzero total momentum \mathbf{Q} is associated with nontrivial spatial structures. In the simplest case of particle-hole pairs with total momentum Q this is a density wave of wave length $\lambda = 2\pi/Q$. In three dimensions, however, we can have several density waves characterized by different momenta \mathbf{Q} . In this case, the resulting spatial structure is a crystal. In general, the p - h pairing gap can be written as

$$\sigma(\mathbf{r}) = \sum_j \sum_{n=-\infty}^{+\infty} \sigma_{j,n} e^{in\mathbf{Q}_j \cdot \mathbf{r}}, \quad (33)$$

where the \mathbf{Q}_j correspond to the (finite) number of fundamental waves, and the summation over $|n| > 1$ accounts for higher harmonics in the Fourier series. The matrix propagator formalism allows for the treatment of more than one density wave through a straightforward expansion of the basis states according to

$$\hat{G} = \begin{pmatrix} \langle c_{k\uparrow} c_{k\uparrow}^\dagger \rangle & \langle c_{k\uparrow} c_{k+Q_x\downarrow}^\dagger \rangle & \langle c_{k\uparrow} c_{k+Q_y\downarrow}^\dagger \rangle & \cdots \\ \langle c_{k+Q_x\downarrow} c_{k\uparrow}^\dagger \rangle & \langle c_{k+Q_x\downarrow} c_{k+Q_x\downarrow}^\dagger \rangle & \langle c_{k+Q_x\downarrow} c_{k+Q_y\downarrow}^\dagger \rangle & \cdots \\ \langle c_{k+Q_y\downarrow} c_{k\uparrow}^\dagger \rangle & \langle c_{k+Q_y\downarrow} c_{k+Q_x\downarrow}^\dagger \rangle & \langle c_{k+Q_y\downarrow} c_{k+Q_y\downarrow}^\dagger \rangle & \cdots \\ \vdots & \vdots & \vdots & \ddots \end{pmatrix}. \quad (34)$$

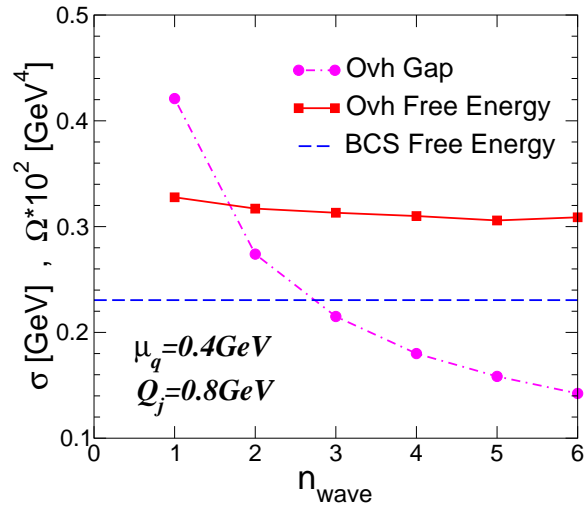


Fig. 2. Dependence of the free energy (upper full line) and p - h pairing gap (dashed-dotted) on the number of waves ('patches') with fixed magnitude of the three-momentum $|Q_j| = 0.8$ GeV. The full line shows the value of the BCS ground state free energy. The results correspond to an instanton calculation with $\mu_q = 0.4$ GeV and $N/V = 1 \text{ fm}^{-4}$.

The possibility of simultaneous BCS pairing can be incorporated by extending the Gorkov propagator to include both particle-hole and particle-particle components. In the following we will consider up to $n_w = 6$ waves in three orthogonal directions with $Q_x = Q_y = Q_z$ and $n = \pm 1$, characterizing a cubic crystal.

Note that in the propagators G_0 we do not include the contribution of anti-particles. This should be a reasonable approximation in the quark matter phase at sufficiently large μ_q , when the standard particle-anti-particle chiral condensate has disappeared. At the same time, since our analysis is based on non-perturbative forces, the range of applicability is limited from above. Taken together, we estimate the range of validity for our calculations to be roughly given by $0.4 \text{ GeV} \gtrsim \mu_q \gtrsim 0.6 \text{ GeV}$. This coincides with the regime where, for the physical current strange quark mass of $m_s \simeq 0.14$ GeV, the two-flavor superconductor might prevail over the color-flavor locked (CFL) state so that our restriction to $N_f = 2$ is supported.

Solutions of the gap equations correspond to extrema (minima) in the energy density with respect to the gap σ . However, solutions may exist for several values of the wave vector Q . To determine the minimum in this quantity, one has to take into account the explicit form of the free energy density. In the mean-field approximation,

$$V_3 \Omega(\mu_q, Q, \sigma) = \int d^3x \left(\frac{\sigma^2(x)}{2\lambda} + \langle q^\dagger (i\alpha \cdot \nabla - 2\sigma(x)q) \rangle \right), \quad (35)$$

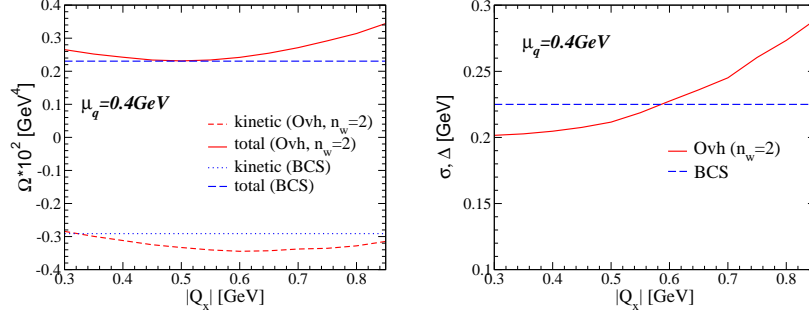


Fig. 3. Left panel: wave-vector dependence of the density wave free energy for one standing wave (full line: Ω_{tot}^{Ovh} , short-dashed line: Ω_{kin}^{Ovh}) in comparison to the BCS solution (long-dashed line: Ω_{tot}^{BCS} , dotted line: Ω_{kin}^{BCS}) at $\mu_q = 0.4\text{GeV}$. Right panel: wave-vector dependence of the density wave pairing gap (full line) compared to the BCS gap (long-dashed line).

where V_3 is the 3-volume. The first contribution removes the double counting from the fermionic contribution in the mean-field treatment.

We have studied the coupled gap equations numerically. We do not find any solutions with simultaneous particle-particle and particle-hole condensates. This reduces the problem to the question whether the BCS or the density wave state is thermodynamically favored. The BCS solution $\Delta = 0.225\text{ GeV}$ is unique and has free energy of $\Omega_{BCS}(\mu_q = 0.4\text{ GeV}) = 2.3 \cdot 10^{-3}\text{ GeV}^4$. Here, we have neglected an irrelevant overall constant that does not affect the comparison with the density wave state.

The situation is more complicated in the case of particle-hole pairing. Let us start with the 'canonical' case where the momentum of the chiral density wave is fixed at twice the Fermi momentum, $Q = 2p_F$. In fig. 2 the resulting minimized free energy is displayed as a function of the number of included waves. The density wave solutions are not far above the BCS groundstate, with a slight energy gain for an increased number of waves.

However, one can further economize the energy of the chiral density wave state by exploiting the freedom associated with the wave vector Q (or, equivalently, the periodicity of the lattice). For $Q > 2p_F$ the free energy rapidly increases. On the other hand, for $Q < 2p_F$ more favorable configurations are found. To correctly assess them one has to include the waves in pairs $|k \pm Q_j|$ of standing waves ($n_w = 2, 4, 6, \dots$) to ensure that the occupied states in the Fermi sea are saturated within the first Brillouin Zone. The lowest-lying state we could find at $\mu_q = 0.4\text{ GeV}$ occurs for one standing wave with $Q_{min} \simeq 0.5\text{ GeV}$ and $\sigma \simeq 0.21\text{ GeV}$ with a free energy $\Omega \simeq 2.3 \cdot 10^{-3}\text{ GeV}^4$, practically degenerate with the BCS solution. This density wave has a wavelength $\lambda \simeq 2.5\text{ fm}$. The minimum in the wave vector is in fact rather shallow, as seen from the explicit momentum dependence of the free energy displayed in fig. 3.

6 Acknowledgements

We would like to thank our collaborators R. Rapp, M. Velkovsky, F. Wilczek and I. Zahed.

References

1. S. C. Frautschi, Asymptotic freedom and color superconductivity in dense quark matter, in: Proceedings of the Workshop on Hadronic Matter at Extreme Energy Density, N. Cabibbo, Editor, Erice, Italy (1978).
2. B. C. Barrois, Nucl. Phys. **B129**, 390 (1977).
3. F. Barrois, Nonperturbative effects in dense quark matter, Ph.D. thesis, Caltech, UMI 79-04847-mc (microfiche).
4. D. Bailin and A. Love, Phys. Rept. **107**, 325 (1984).
5. N. Evans, S. D. Hsu and M. Schwetz, Nucl. Phys. **B551**, 275 (1999) [hep-ph/9808444].
6. N. Evans, S. D. Hsu and M. Schwetz, Phys. Lett. **B449**, 281 (1999) [hep-ph/9810514].
7. T. Schäfer and F. Wilczek, Phys. Lett. **B450**, 325 (1999) [hep-ph/9810509].
8. W. E. Brown, J. T. Liu and H. Ren, Phys. Rev. **D62**, 054016 (2000) [hep-ph/9912409].
9. T. Schäfer, Phys. Rev. **D62**, 094007 (2000) [hep-ph/0006034].
10. M. Alford, K. Rajagopal and F. Wilczek, [hep-ph/9711395].
11. R. Rapp, T. Schäfer, E. V. Shuryak and M. Velkovsky, Phys. Rev. Lett. **81**, 53 (1998) [hep-ph/9711396].
12. D. T. Son, Phys. Rev. **D59**, 094019 (1999) [hep-ph/9812287].
13. T. Schäfer and F. Wilczek, Phys. Rev. **D60**, 114033 (1999) [hep-ph/9906512].
14. R. D. Pisarski and D. H. Rischke, Phys. Rev. **D61**, 074017 (2000) [nucl-th/9910056].
15. D. K. Hong, V. A. Miransky, I. A. Shovkovy and L. C. Wijewardhana, Phys. Rev. **D61**, 056001 (2000) [hep-ph/9906478].
16. W. E. Brown, J. T. Liu and H. Ren, Phys. Rev. **D61**, 114012 (2000) [hep-ph/9908248].
17. T. Schäfer, Nucl. Phys. **B575**, 269 (2000) [hep-ph/9909574].
18. N. Evans, J. Hormuzdiar, S. D. Hsu and M. Schwetz, Nucl. Phys. **B581**, 391 (2000) [hep-ph/9910313].
19. M. Alford, K. Rajagopal and F. Wilczek, Nucl. Phys. **B537**, 443 (1999) [hep-ph/9804403].
20. T. Schäfer and F. Wilczek, Phys. Rev. Lett. **82**, 3956 (1999) [hep-ph/9811473].
21. M. Alford, J. Berges and K. Rajagopal, Nucl. Phys. **B558**, 219 (1999) [hep-ph/9903502].
22. T. Schäfer and F. Wilczek, Phys. Rev. **D60**, 074014 (1999) [hep-ph/9903503].
23. P. Bedaque, hep-ph/9910247.
24. M. Alford, J. Bowers and K. Rajagopal, hep-ph/0008208.
25. A. B. Migdal, Sov. Phys. JETP **36**, 1052 (1973).
26. R. F. Sawyer, Phys. Rev. Lett. **29**, 382 (1972).
27. D. J. Scalapino, Phys. Rev. Lett. **29**, 392 (1972).
28. D. B. Kaplan and A. E. Nelson, Phys. Lett. **B175**, 57 (1986).
29. G. E. Brown, K. Kubodera, and M. Rho, Phys. Lett. **B175**, 57 (1987).

30. T. Schäfer, nucl-th/0007021.
31. R. Casalbuoni and D. Gatto, Phys. Lett. **B464**, 111 (1999) [hep-ph/9908227].
32. D. T. Son and M. Stephanov, Phys. Rev. **D61**, 074012 (2000) [hep-ph/9910491],
erratum: hep-ph/0004095.
33. M. Rho, A. Wirzba, and I. Zahed, Phys. Lett. **B473**, 126 (2000) [hep-ph/9910550].
34. D. K. Hong, T. Lee, and D. Min, Phys. Lett. **B477**, 137 (2000) [hep-ph/9912531].
35. C. Manuel and M. H. Tytgat, Phys. Lett. **B479**, 190 (2000) [hep-ph/0001095].
36. S. R. Beane, P. F. Bedaque, and M. J. Savage, Phys. Lett. **B483**, 131 (2000)
[hep-ph/0002209].
37. D. V. Deryagin, D. Yu. Grigoriev, and V. A. Rubakov, Int. J. Mod. Phys. **A7**, 659
(1992).
38. E. Shuster and D. T. Son, Nucl. Phys. **B573**, 434 (2000) [hep-ph/9905448].
39. R. Rapp, E. Shuryak and I. Zahed, hep-ph/0008207.